



# Parametric Study on Fatigue Failure Modes of the Rib-Deck Weld Under Out-of-Plane Bending Loading

Wang Qiu-dong<sup>1</sup> · Wei Yang<sup>1</sup> · Fu Zhong-qiu<sup>2</sup> · Wang Yi-xun<sup>3</sup>

Received: 19 August 2022 / Accepted: 21 February 2023 / Published online: 6 March 2023  
© The Author(s), under exclusive licence to Shiraz University 2023

## Abstract

To clarify the factors affecting the fatigue failure mode of the rib-deck weld, the parameter  $\lambda$  defined by the ratio of the effective notch stress range ( $\Delta\sigma_0$ ) to the corresponding fatigue strength ( $\Delta\sigma_R$ ) is proposed to predict the failure mode. Three types of fatigue tests were reviewed to validate the proposed method. On this basis, finite element modeling and parametric analysis were conducted to investigate the effects of the loading mode, boundary condition, weld geometry and stress ratio on the potential failure mode. Finally, fatigue testing programs for generating objective failure modes were analyzed and suggested. Results show that the proposed method is feasible to predict the potential failure mode of the rib-deck weld under out-of-plane bending moment. The fatigue failure mode is considerably affected by the loading mode, boundary condition and stress ratio. In terms of the geometric parameters of the weld, only the weld leg length at deck plate ( $l_{w,d}$ ) and thickness of the deck plate ( $t_d$ ) have a minor influence, while the other parameters possess no effect. Suggestions for the fatigue testing programs for generating the root-deck, toe-deck, root-weld and toe-rib failure modes are proposed, which is of valuable reference meaning for further experimental investigations.

**Keywords** Orthotropic steel deck · Rib-deck weld · Fatigue failure mode · Effective notch stress · Parametric analysis

## 1 Introduction

The orthotropic steel deck (OSD) has been widely used since the twentieth century (Dowling 1992). The OSD is easily subjected to fatigue cracking due to the effects of weld notch,

welding residual stress, short stress influence lines and some other factors (Wang et al. 2019a, b; Kolstein 2007). There are many types of fatigue cracks in the OSD (Kolstein 2007; Ji et al. 2013; Xiao et al. 2008), e.g., the rib-deck weld crack, butt weld crack, diaphragm-rib weld crack, etc. Among them, the rib-deck crack has raised great concern in recent years, since there further exist four types of fatigue cracks (Figs. 1 and 2) which makes the fatigue mechanism more complex (Kolstein 2007; Fish and Barsom 2015). To the best knowledge of the authors, the toe-deck crack, root-deck crack and root-weld crack have been observed in both practical engineering and laboratory tests, while the toe-rib crack is only detected in a few fatigue tests (see Fig. 2).

Full-scale and local-scull fatigue tests including various geometric sizes, loading modes and boundary conditions have been carried out to evaluate the fatigue performance of rib-deck welds. Sim et al. (2012), Kainuma et al. (2017), Heng et al. (2017) and Freitas et al. (2017) carried out the fatigue tests of full-scale OSDs to evaluate the fatigue performance of rib-deck welds. Both root-deck crack and toe-deck crack are observed in these fatigue tests. However, due to the limitations of test site, loading equipment, financial matter, etc., it is difficult to extensively carry out

✉ Wei Yang  
wy78@njfu.edu.cn

Wang Qiu-dong  
qdwang@njfu.edu.cn

Fu Zhong-qiu  
fuzhongqiu@hhu.edu.cn

Wang Yi-xun  
y.wang@civil.eng.osaka-u.ac.jp

<sup>1</sup> College of Civil Engineering, Nanjing Forestry University, No.159 Longpan Road, Xuanwu District, Nanjing 210037, Jiangsu Province, People's Republic of China

<sup>2</sup> College of Civil and Transportation Engineering, Hohai University, No.1 Xikang Road, Gulou District, Nanjing 210098, Jiangsu Province, People's Republic of China

<sup>3</sup> Department of Civil Engineering, Osaka University, 1-1 Yamadaoka, Suita, Osaka 565-0871, Japan

**Fig. 1** Fatigue cracks of rib-deck welds in practical engineering

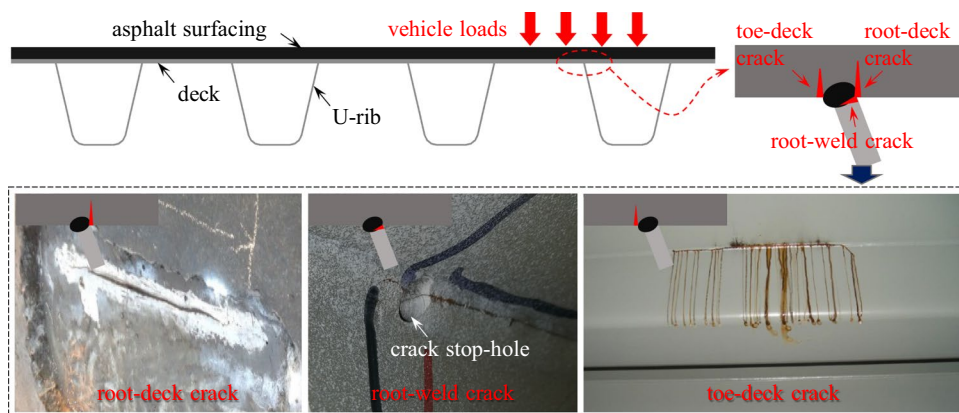
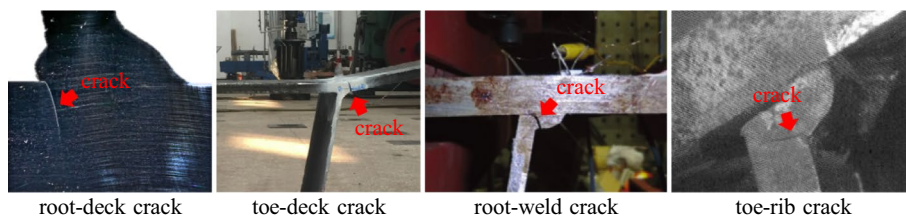


**Fig. 2** Fatigue cracks of rib-deck welds in fatigue tests



the full-scale fatigue test. Most researchers have adopted the local-scale fatigue test as an alternative to investigate the fatigue performance of rib-deck welds. Maddox (1974), Yamada et al. (2008), Fu et al. (2017, 2018), Ya et al. (2011) and Chen et al. (2014) conducted a series of fatigue tests of local-scale rib-deck welded specimens with open ribs. In these fatigue tests, root-deck cracks are most commonly observed, subsequently toe-deck cracks. Meanwhile, many researchers focused on the fatigue test of local-scale rib-deck welded specimens with closed U-ribs, such as Maddox (1974), Bruls (1990), Bignonnetl et al. (1990), Li et al. (2018), Chen et al. (2014), Cao et al. (2019), Zhao et al. (2010), Tian et al. (2011), Wang et al. (2021a, b) and some others. In these fatigue tests, toe-deck cracks are most commonly observed, while the root-deck crack, root-weld crack and toe-rib crack were only observed by Wang et al. (2021a, b), Li et al. (2018) and Tian et al. (2011), respectively. In general, it could be concluded that the toe-deck and root-deck failure modes could be achieved by either full-scale or local-scale fatigue tests; however, specific test program for obtaining root-weld and toe-rib failure modes remains unclear.

The main purpose of conducting fatigue tests is to propose a unified  $S-N$  curve for fatigue damage assessment, *i.e.*, fatigue life prediction. When employing the Miner's rule (Schijve 2009), the fatigue strength corresponding to a fatigue failure life ( $N_f$ ) of 2 million cycles is necessary. In terms of the rib-deck weld, a fatigue strength of 71 MPa is recommended by the IIW (Hobbacher 2016) and Eurocode (2005), and 69 MPa recommended by the AASHTO (2004). The code-recommended fatigue

strength is feasible for anti-fatigue design (Wang et al. 2022); however, regarding to the fatigue life prediction of a serviced steel bridge, referring to the code-recommended values may lead to inaccurate results. The reason is that the values of fatigue strength corresponding to each fatigue failure mode of rib-deck weld differ from each other. For example, a series of fatigue testing data (Wang et al. 2022) were reviewed and re-analysed in the nominal stress system, as plotted in Fig. 3, where the parameter  $T_\sigma$  was used as the indication of the evaluation reliability, which was determined by the reciprocal of the ratio of the fatigue strength at  $P_s = 2.3\%$  and 97.7%. It could be found that the regressed fatigue strength corresponding to the root-deck failure is 71.4 MPa, which is close to the values recommended by the IIW, Eurocode and AASHTO; however, the regressed values corresponding to the toe-deck, root-weld and toe-rib failure are 93.2, 85.1 and 101 MPa, respectively. It indicates that when a serviced bridge subjected to one of the failure modes excluding the root-deck failure (e.g., the Jiangyin Yangtze River Bridge subjected to the root-weld cracks Rao et al. 2019) is assessed, referring to the code-recommended fatigue strength will lead to inaccurate prediction results. Instead, the fatigue strength corresponding to relative failure mode should be referred to; however, only a few fatigue testing data corresponding to the root-weld and toe-rib failure modes are available in current literatures, which is not enough to propose reliable values of fatigue strength. The fundamental reason is that the fatigue mechanism of the root-weld and toe-rib failure modes is unclear, making it difficult to develop specific test program to obtain the

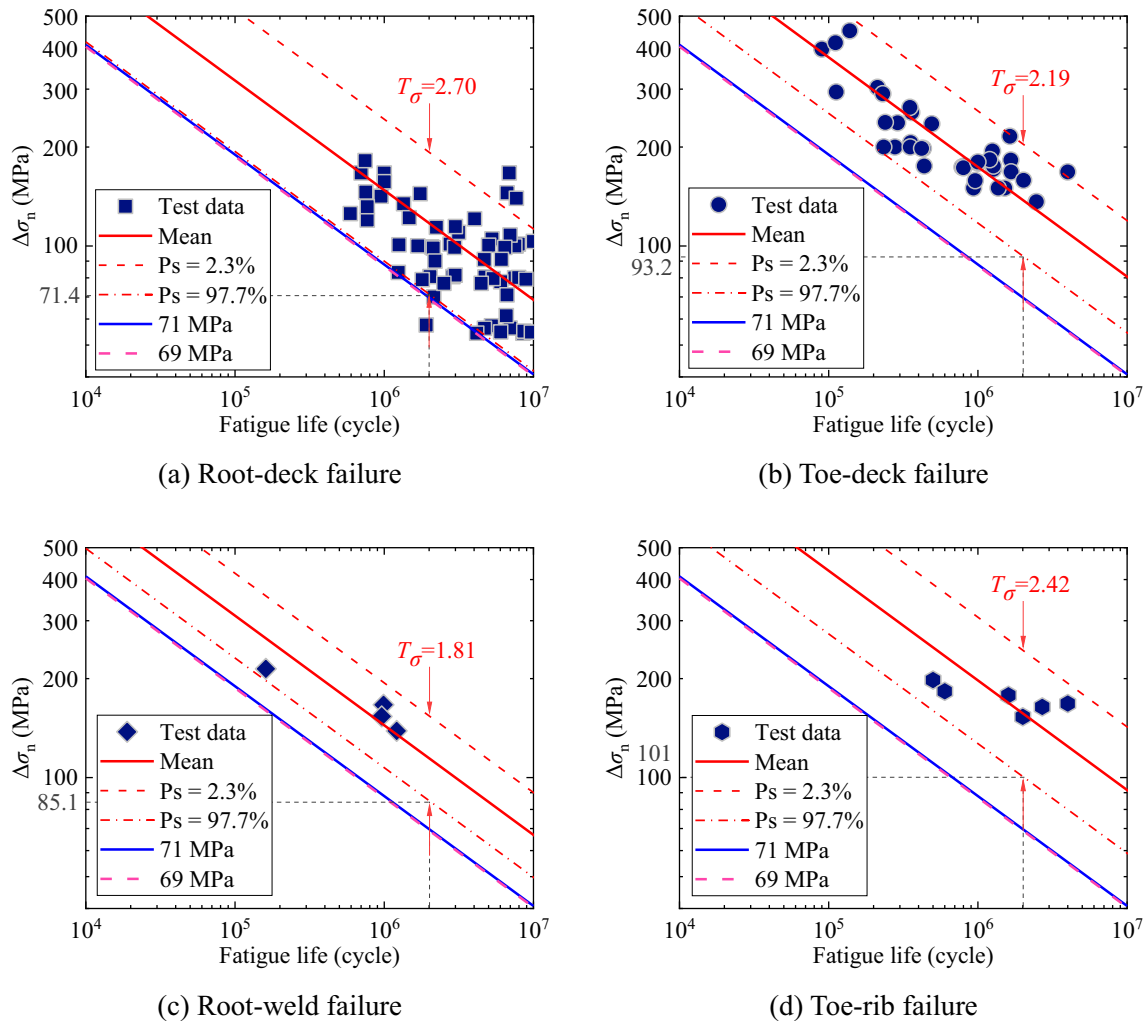


**Fig. 3** Regressed fatigue strength of the rib-deck weld corresponding to different failure modes

root-weld and toe-rib cracks. Investigating the factors affecting the fatigue failure mode of the rib-deck weld is essential for developing the fatigue test program corresponding to specific failure mode, which warrants further research.

In this study, the method integrating the effective notch stress approach was proposed and validated for predicting the fatigue failure modes of the rib-deck weld. Parametric analyses were comprehensively performed to investigate the effect of the loading mode, boundary condition, weld geometry (i.e., the weld penetration rate, thicknesses of the deck plate and U-rib, lengths of the weld leg and the angle between deck plate and rib wall) and stress ratio on the fatigue failure mode of the rib-deck weld. On this basis, suggestions for fatigue test schemes were proposed to specifically generate four types of fatigue failure modes of the rib-deck weld.

## 2 Method for Predicting the Fatigue Failure Mode

It is believed that both crack initiation position and initial propagation path could be predicted by employing the effective notch stress (ENS) approach (Wang et al. 2019a, b). The ENS approach is a local stress-based numerical fatigue approach (Radaj 1996), and the basic idea of the method comes from Neuber's micro-support hypothesis (Radaj et al. 2013), of which the basis is that the calculated stress at the crack tip is proportional to the reciprocal of the square root of crack tip radius using linear-elastic theory (Sonsino et al. 2012). The ENS approach recommended by IIW is using a reference radius of 1 mm and applying the first principal stress. The fatigue critical point and maximum principal stress could be obtained by

the ENS approach, which has the potential to predict the crack initiation position and the propagation path, i.e., the fatigue failure mode.

For verification, the fatigue test conducted by Fu et al. (2017) was simulated by the ANSYS software, as shown in Fig. 4. The boundary condition, loading mode and geometry of the finite element (FE) model were kept the same with the test scheme (Wang et al. 2019a, b). Rib-deck welded specimens with 80% and 100% penetration rates (i.e., labelled P80 and P100) were simulated in the present study. All FE models were simulated by SOLID186-typed elements which is defined by 20 nodes having three degrees of freedom each. The Young modulus ( $E$ ) and Poisson ratio ( $\nu$ ) of the steel material were set as 206 GPa and 0.3, respectively. A round notch with a radius of 1 mm was arranged at the weld root following the recommendations by the IIW, and the first principal stress ( $\sigma_1$ ) was taken as the effective notch stress here. For details of the mesh sensitivity analysis, please refer to Wang et al. (2019a, b). For giving consideration to both the solving accuracy and computing efficiency, transition regions of the meshing size were arranged around the notch and the notch edge was divided into 40 equal parts (Wang et al. 2021a, b).

The angle embedded in Fig. 4 represents the crack propagation direction after crack initiation. It could be seen that the angle representing the crack propagation path is  $6^\circ$  and  $13^\circ$  for P80 and P100 respectively, which is similar to the experimental results (i.e.,  $7^\circ$  and  $16^\circ$ ). The minor differences could be attributed to the effect of the welding residual stress which is not considered in the FE analysis.

After verifying the feasibility of predicting the crack initiation position using the effective notch stress approach, it is essential to develop a method to determine the potential one out of four types of fatigue failure modes. In this study, a dimensionless parameter ( $\lambda$ ) was defined to predict the potential fatigue failure mode. The  $S$ – $N$  curve could be taken as the form expressed by Eq. (1) (Hobbacher 2016). Given arbitrary stress range  $\Delta\sigma_0$ , the corresponding fatigue life ( $N_0$ ) could be obtained using Eq. (2). It is obvious that the potential fatigue crack will initiate at the position which

is with the smallest value of  $N_0$ . On this basis, the parameter  $\lambda$  defined by Eq. (3) is proposed to determine the potential fatigue failure mode. It is obvious that fatigue crack will initiate at the position with the greatest value of  $\lambda$ .

$$C = N \times (\Delta\sigma)^m \quad (1)$$

$$N_0 = N_f \times (\Delta\sigma_R)^m / (\Delta\sigma_0)^m \quad (2)$$

$$\lambda = \sqrt[m]{N_f/N_0} = \Delta\sigma_0/\Delta\sigma_R \quad (3)$$

where  $C$  is a constant;  $N$  is fatigue life in cycles;  $m$  is an exponent of  $S$ – $N$  curve;  $\Delta\sigma$  and  $\Delta\sigma_0$  are stress ranges;  $N_0$  is the fatigue life corresponding to  $\Delta\sigma_0$ ;  $\Delta\sigma_R$  is the fatigue strength;  $N_f$  is the fatigue failure life. Notably, the effects of the uncertainties of weld defects and residual stresses are implicit in the fatigue strength ( $\Delta\sigma_R$ ), thus the differences are not considered. In future studies, it is meaningful to develop the probabilistic model to describe such uncertainties, to further improve the accuracy of the predicting accuracy of the failure mode.

### 3 Validation of the Proposed Method

#### 3.1 Review of Fatigue Tests

To validate the feasibility of the proposed method, fatigue tests of rib-deck welded specimens (Li et al. 2018; Cheng et al. 2017; Tian et al. 2011) were referred to. The specimens' geometry, loading conditions and fatigue failure modes were plotted in Fig. 5. Specimens with 15% and 75% penetration rates were tested under a stress ratio ( $R$ ) of  $-1$  (Li et al. 2018). Root-weld cracks were observed in 15%-penetrated specimens and toe-deck cracks in 75%-penetrated specimens, as hinted in Fig. 5a. Specimens with a penetration rate of 80% were tested under  $R=0.1$  (Cheng et al. 2017), generating toe-deck cracks (see Fig. 5b). Both full-penetrated and non-penetrated specimens were tested

**Fig. 4** Feasibility validation for predicting the crack initiation position by the effective notch stress approach, where P80 and P100 stand for 80% and 100% penetration, respectively. (Unit: mm)

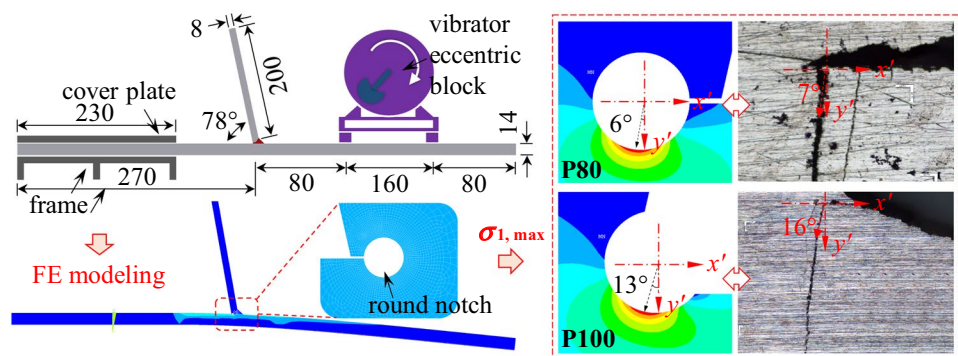


**Fig. 5** Specimens' geometry, loading conditions and fatigue failure modes of cited fatigue tests (Unit: mm)

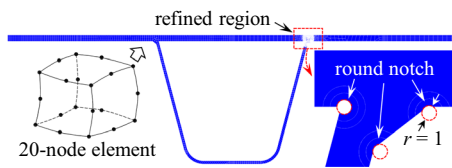
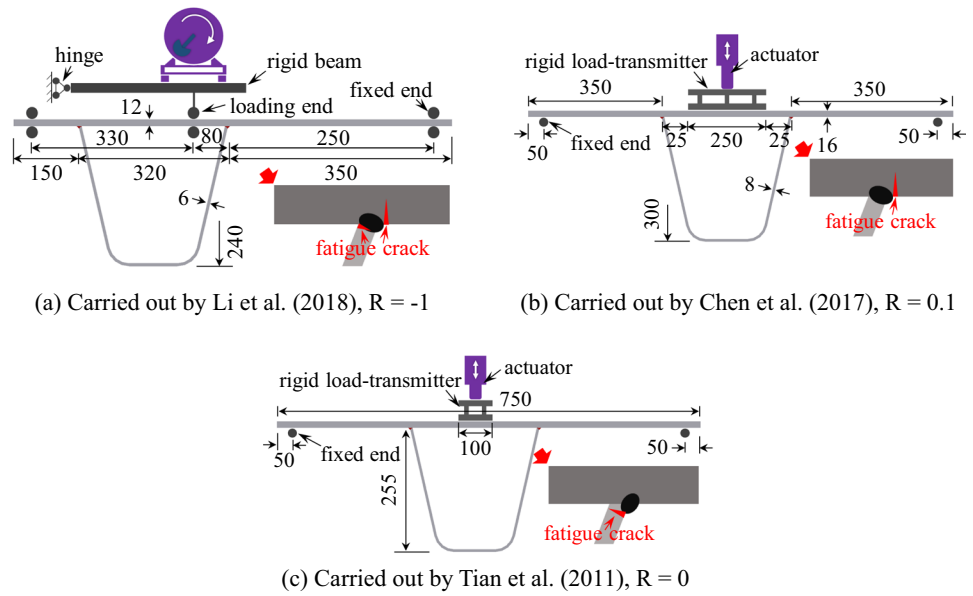


**Fig. 6** Taking specimen adopted by Chen et al. (2014) for example, the FE model and arrangement of round notches (Unit: mm)

under  $R = 0$  (Tian et al. 2011), and toe-rib cracks were observed in the latter one (see Fig. 5c) which is referred to.

### 3.2 Finite Element Modeling and Validation

FE models corresponding to the abovementioned fatigue tests were developed. Taking the FE model simulating the fatigue test conducted by Chen et al. (2014) for example, three round notches with a radius of 1 mm were arranged at the weld root and weld toe respectively, as shown in Fig. 6. In this case, the effective notch stresses at four potential crack initiation positions could be obtained simultaneously, subsequently determining the values of  $\lambda$ . The parameters of developed FE modes were kept the same with the model introduced in Sect. 2.

The effective notch stress nephograms were shown in Fig. 7. In view that the 80%- and non-penetrated specimens were tested under  $R = 0.1$  and 0, it could be concluded from Fig. 7a, d that the root-weld crack will not be generated when subjected to a positive stress ratio. Meanwhile, obvious notch stress concentrations are found at the notch edge corresponding to the other three types of cracks, which will be adopted for determining the parameter  $\lambda$  in the following

section. It can be seen from Fig. 7b, c that severe stress concentrations are observed in the notch edge corresponding to the root-weld crack when subjected to  $R = -1$ , especially for the 15%-penetrated FE model.

The effective notch stress range ( $\Delta\sigma_1$ ) was obtained by the FE analysis, then the values of  $\lambda$  were determined by Eq. (3), as plotted in Fig. 8. Notably, the fatigue strength  $\Delta\sigma_R$  was valued 225 MPa according to the IIW. Based on the proposed method, it could be predicted that the toe-deck crack will be generated at 80%- and 75%-penetrated specimens, the root-weld crack generated at 15%-penetrated specimens and the toe-rib crack generated at non-penetrated specimens. The prediction results are fully aligned with the experimental results, which demonstrates that the proposed method is feasible and reliable to predict the fatigue failure mode of the rib-deck weld.

## 4 Parametric Analyses

### 4.1 FE model for parametric analysis

To investigate the factors affecting the fatigue failure mode, parametric analyses were performed. Figure 9 shows the schematic diagram of the FE model which has a length of  $3 \times L_d$  and a width of  $W_d$ . In this study,  $L_d$  and  $W_d$  were set to be 300 and 100 mm, respectively. The height of the U-rib was valued 240 mm. The deck plate thickness ( $t_d$ ), rib thickness ( $t_r$ ), weld penetration rate ( $1 - t_p/t_r$ ), weld leg length at deck plate ( $l_{w,d}$ ), weld leg length at rib wall ( $l_{w,r}$ ) and the angle between the deck plate and rib wall ( $\theta$ ) were assigned different values for parametric analyses, as to be introduced in the following sections. Different loading modes and

**Fig. 7** Effective notch stress ( $\sigma_1$ ) nephograms

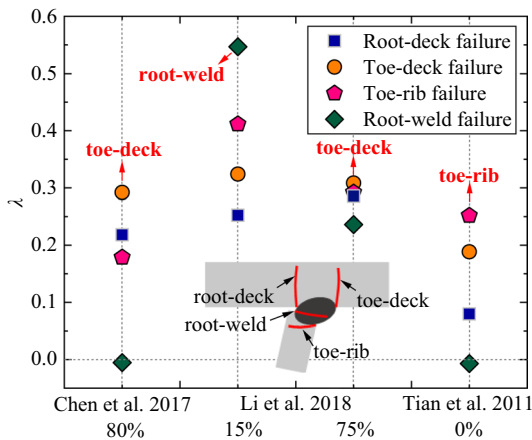
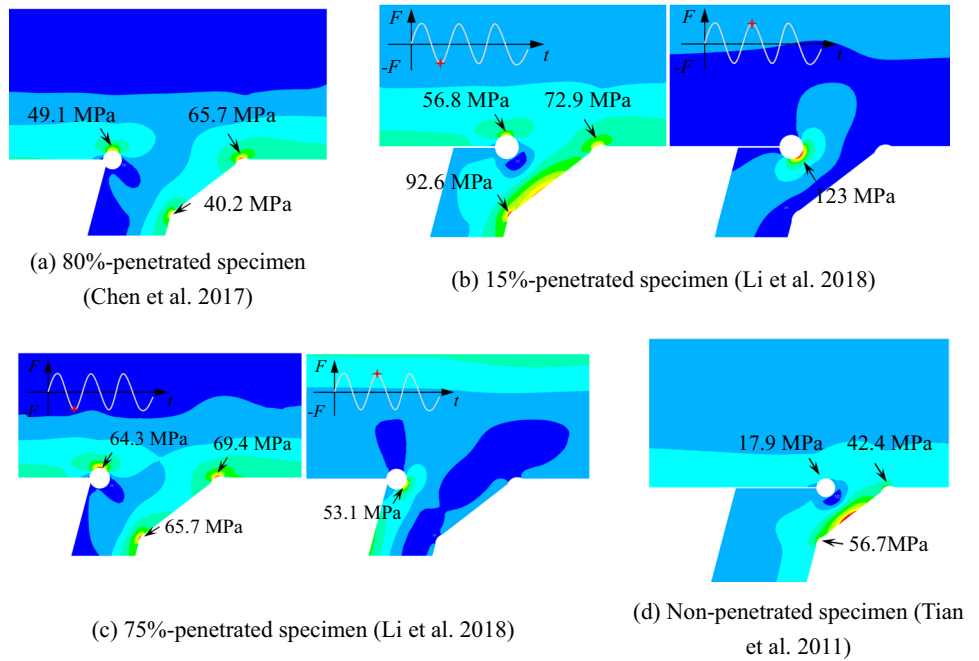
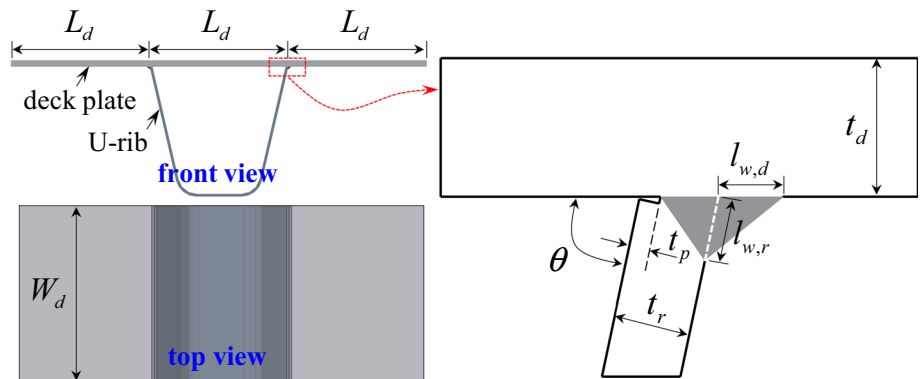


**Fig. 8** Comparison of the numerical and experimental results of the failure modes

**Fig. 9** Schematic diagram of the FE model



boundary conditions were also considered for parametric analysis. The arrangement of the notches and parameters of the FE model were kept the same with the abovementioned FE models.

### 4.2 Effect of the Loading Mode

The loading modes commonly employed in fatigue tests could be categorized into five types (labelled loading mode I, II, III, IV and V, see Fig. 10), which were considered in the following parametric analysis. The boundary condition, loading position and applied surface loads were also shown in Fig. 10. The geometric sizes of the FE model were valued as follows:  $t_r=6$  mm,  $t_d/t_r=2.0$ ,  $l_{w,d}/t_r=l_{w,r}/t_r=1.0$ ,  $\theta=75^\circ$ . And the stress ratio was set to be 0 here.

**Fig. 10** Loading modes considered in the FE analysis, where the black block on the left side of the specimen represents fixed end (i.e.,  $U_x = U_y = U_z = 0$ ) and the black circle on the other side represents simply supported end (i.e.,  $U_y = U_z = 0$ )

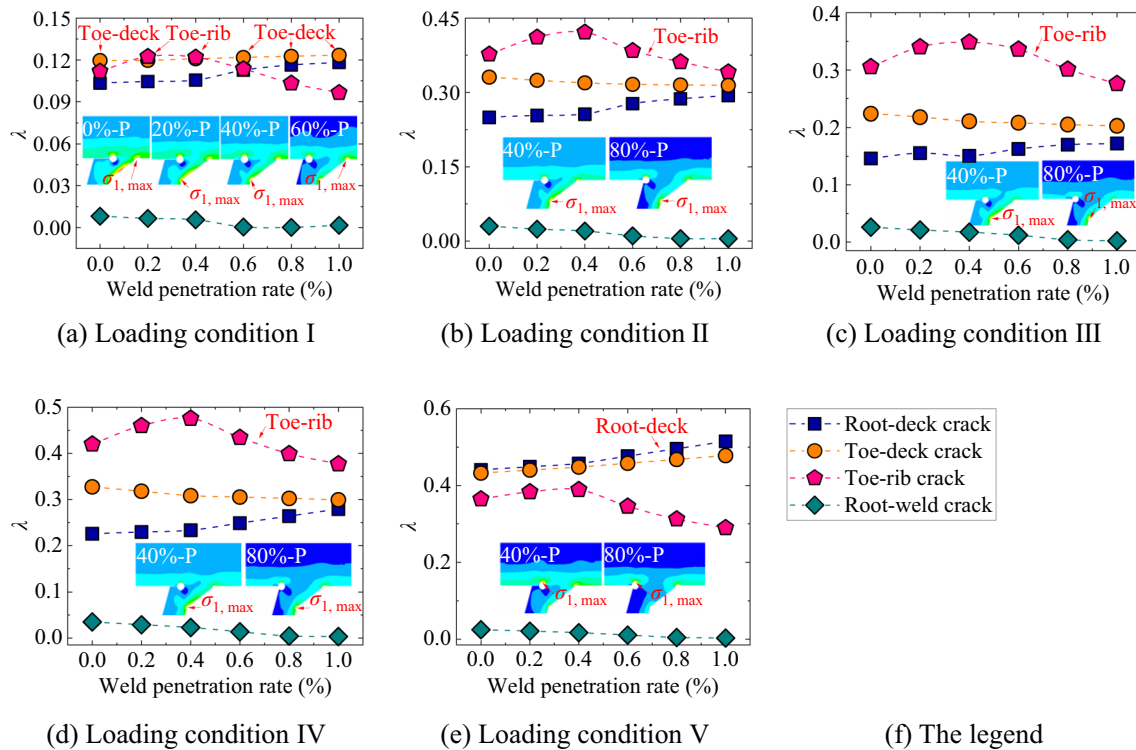
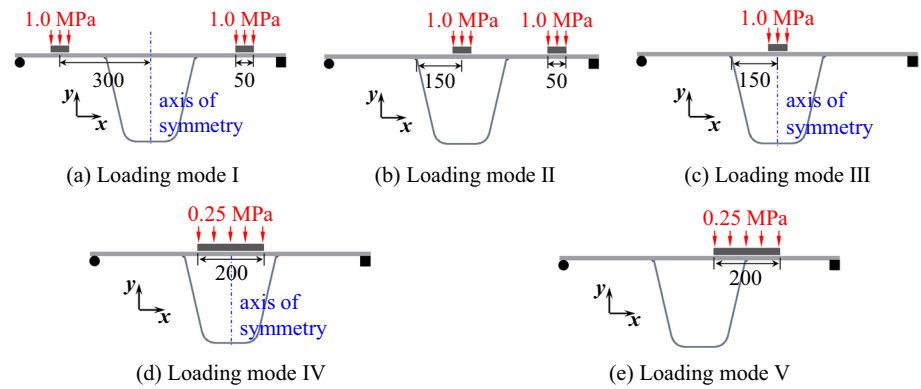


**Fig. 11** Effect of the loading mode on the value of  $\lambda$  in presence of different weld penetration rates, where  $t_r = 6$  mm,  $t_d/t_r = 2.0$ ,  $l_{w,d}/t_r = l_{w,r}/t_r = 1.0$ ,  $\theta = 75^\circ$

Values of  $\lambda$  in presence of different weld penetration rates were plotted in Fig. 11. When the loading mode I is adopted, the concentration position of the maximum principal stress ( $\sigma_{1,max}$ ) is significantly affected by the weld penetration rate (Fig. 11a): the position of  $\sigma_{1,max}$  moves from the deck toe to the rib toe with the weld penetration rate increasing from 0 to 20%, and back to the deck toe as the weld penetration rate exceeding 40%. It indicates that the potential fatigue failure mode is dependent on the weld penetration rate when the loading mode I is employed. However, it can be seen from Figs. 11b–d

that the concentration position of  $\sigma_{1,max}$  remains at the rib toe against the effect of the weld penetration rate, and the value of  $\lambda$  thereat remains largest. It indicates that the toe-rib failure mode will be generated when either one of loading modes II–IV is adopted. Furthermore, the loading mode IV is recommended for efficiency since the value of  $\lambda$  (varying from 0.38 to 0.48) is larger than the one in loading modes II and III. Similarly, Fig. 11e indicates that the root-deck failure mode will be generated when the loading mode V is adopted.

### 4.3 Effect of the Boundary Condition

Eccentric loading modes (*i.e.*, loading modes II and V) were adopted to investigate the effect of the boundary condition. Three types of boundary conditions were considered: (1) boundary condition A, *i.e.*, one side closest to the objective weld was fixed and the other was simply supported; (2) boundary condition B, *i.e.*, one side closest to the objective weld was simply supported and the other was fixed; and (3) boundary condition C, *i.e.*, both sides were fixed. The geometric sizes of developed FE models and applied stress ratio remained unchanged.

Numerical results were plotted in Fig. 12. Similar results are observed in presence of boundary conditions A and C (Fig. 12a, c, d and f), indicating that whether the side away from the objective weld is fixed or not has less effect on the fatigue failure mode. However, in presence of the boundary condition B, greater out-of-plane deformation occurs since the displacement along *x*-axis is not constrained, and potential crack initiation position changes from the rib toe or weld root to the deck toe. In this case, toe-deck failure mode

will be generated instead of the toe-rib and root-deck failure modes (Fig. 12b and e).

### 4.4 Effect of the Weld Geometry

To further investigate the effect of the weld geometry, the loading condition III and boundary condition A were considered in the FE analysis.

The thicknesses of the deck plate and U-rib were valued 12, 16, 20 mm and 6, 8, 10 mm to investigate the effect of plate thickness. It can be seen from Fig. 13a–c that the differences among  $\lambda$  at the weld root, deck toe and rib toe become smaller with increased thickness of the deck plate. In particular, the root-deck failure mode will be generated instead of the toe-rib failure mode at the full-penetrated FE model with  $t_d=20$  mm and  $t_r=6$  mm. However, the potential fatigue failure mode is not affected by the thickness of the rib plate, as shown in Fig. 13a, d and e. Additionally, the value of  $\lambda$  becomes larger in presence of thicker rib plate and thinner deck plate.

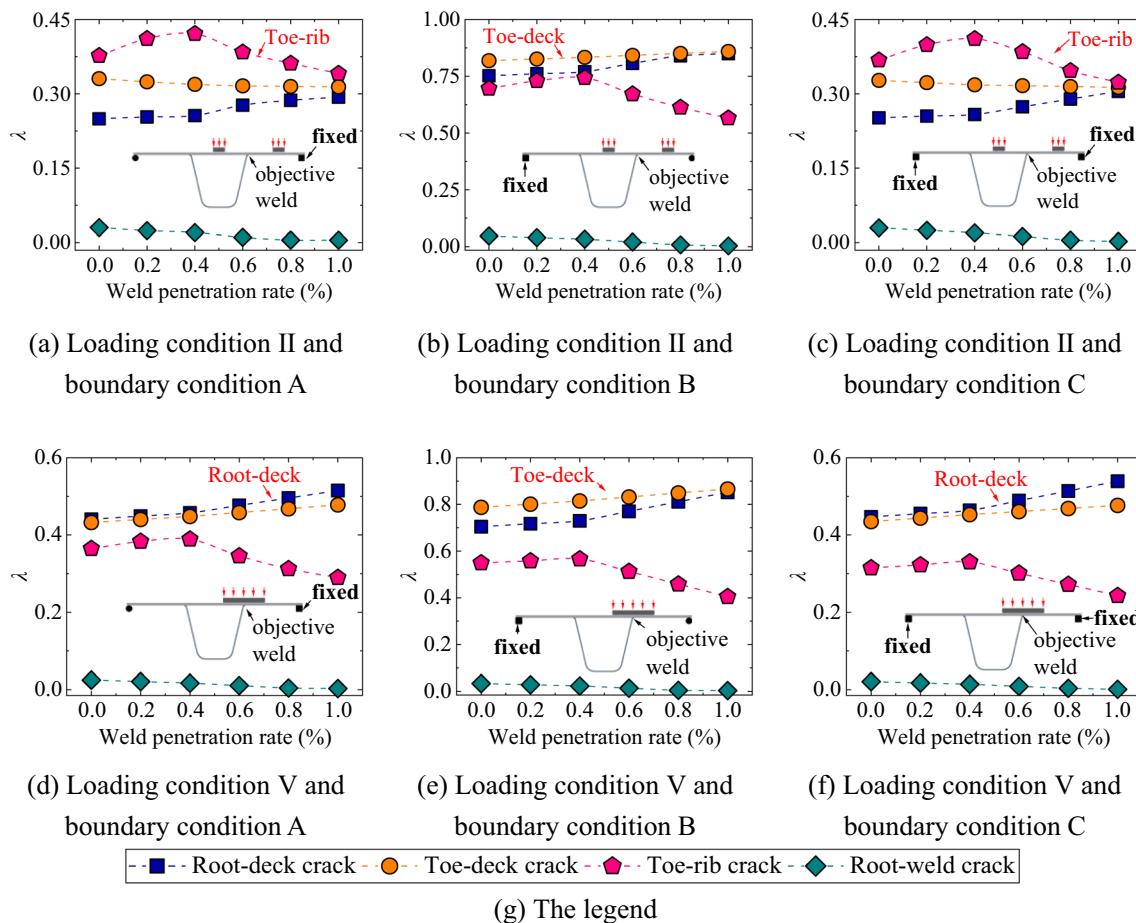


**Fig. 12** Effect of the boundary condition on the value of  $\lambda$  in presence of different weld penetration rates, where  $t_r=6$  mm,  $t_d/t_r=2.0$ ,  $l_{w,d}/t_r=l_{w,r}/t_r=1.0$ ,  $\theta=75^\circ$



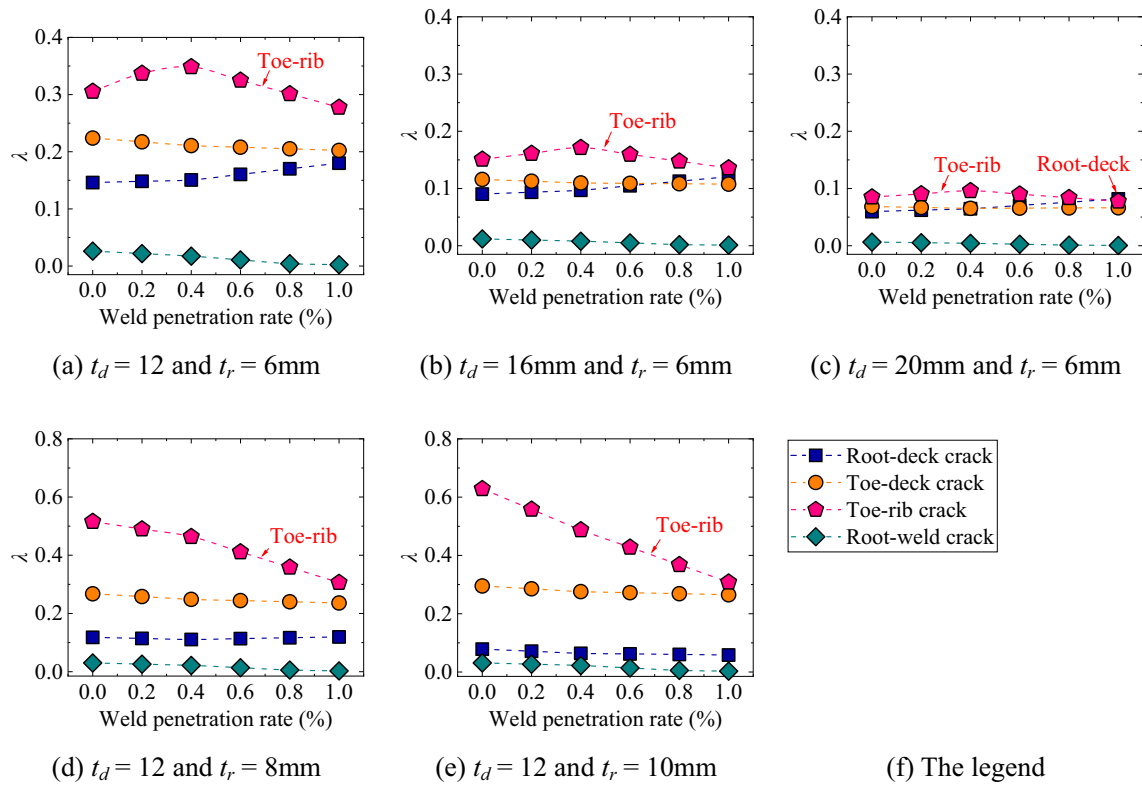


**Fig. 13** Effect of the thicknesses of deck and U-rib plate on the value of  $\lambda$  in presence of different weld penetration rates, where  $l_{w,d}/t_r = l_{w,r}/t_r = 1.0$ ,  $\theta = 75^\circ$

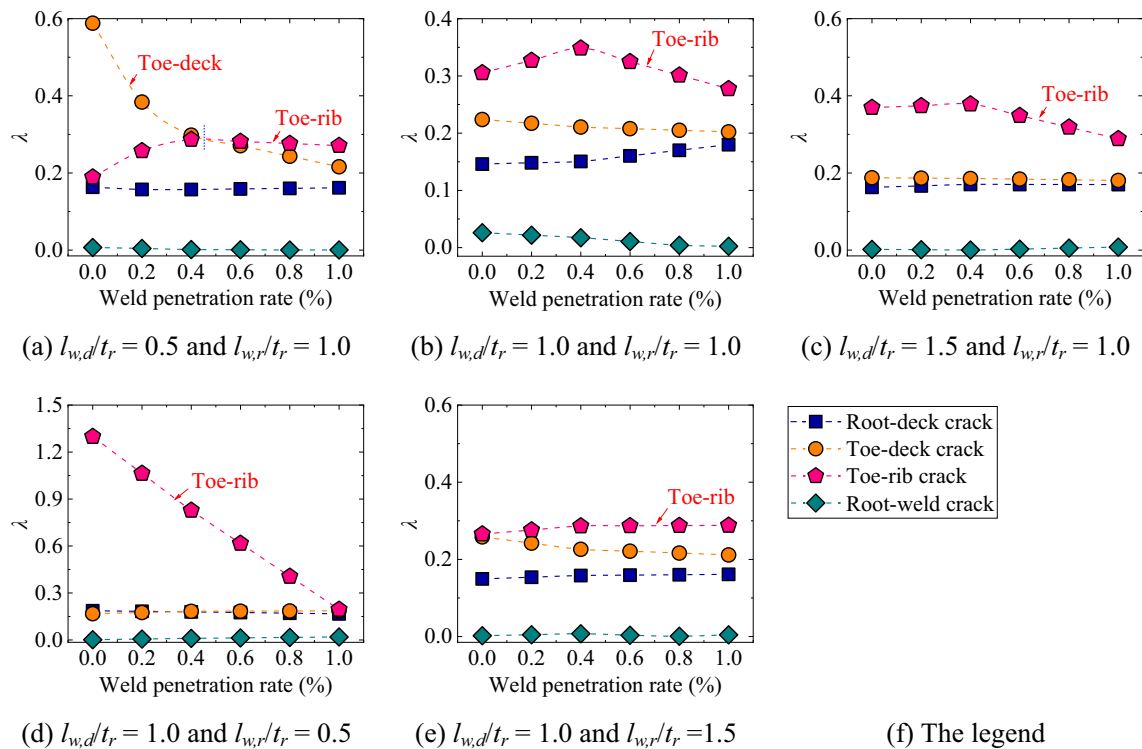


**Fig. 14** Effect of the weld leg length on the value of  $\lambda$  in presence of different weld penetration rates, where  $t_r = 6$  mm,  $t_d/t_r = 2.0$ ,  $\theta = 75^\circ$

To investigate the effect of the weld leg length, the ratio of the weld leg length to the rib thickness (*i.e.*,  $l_{w,d}/t_r$  and  $l_{w,r}/t_r$ ) was valued 0.5, 1.0 and 1.5, respectively. It can be seen from Fig. 14a–c that the value of  $\lambda$  at the deck toe is considerably affected by  $l_{w,d}$ . In presence of  $l_{w,d}/t_r=0.5$  and  $l_{w,r}/t_r=1.0$ , the toe-deck failure mode will be generated when the weld penetration rate is less than 40%. And the toe-rib failure mode will be generated when the weld penetration rate exceeds 40%. When  $l_{w,d}/t_r$  exceeds 1.0, the potential failure mode remains to be the toe-rib failure mode. Additionally, it could be concluded from Fig. 14b, d and e that the potential failure mode is independent on  $l_{w,r}/t_r$ ; however, value of  $\lambda$  becomes larger in presence of smaller  $l_{w,r}/t_r$ , which will make it more efficient to generate toe-rib failure mode in fatigue tests.

Meanwhile, the angle between the deck plate and rib wall ( $\theta$ ) was valued  $70^\circ$ ,  $75^\circ$  and  $80^\circ$  for parametric analysis, and the results were plotted in Fig. 15. It could be seen that the value of  $\lambda$  at the rib toe is mostly affected by the value of  $\theta$ ; however, however, the potential failure mode remains to be the toe-rib failure.

#### 4.5 Effect of the Stress Ratio Induced by External Loading

As stated before, the fatigue failure mode might be also affected by the stress ratio ( $R$ ). In this study,  $R$  was valued  $-1$ ,  $-0.9$ ,  $-0.8$ ,  $-0.5$ ,  $-0.4$ ,  $-0.1$ ,  $0$  and  $0.1$  for parametric analysis, and the results were plotted in Fig. 16.

It can be seen that the variation trend of the values of  $\lambda$  corresponding to the root-deck, toe-deck and toe-rib failure modes is less affected by the stress ratio. Conversely, the value of  $\lambda$  corresponding to the root-weld failure mode becomes larger with the decreased  $R$ , and exceeds the value corresponding to the toe-rib failure mode in presence of a weld penetration rate of 0% when  $R=-0.5$  (Fig. 16e). With

the decreasing  $R$  in presence of low weld penetration rates, the potential fatigue failure mode changes from the toe-rib failure to the root-weld failure (Fig. 16f–h). It could be observed from Fig. 16h that the root-weld failure mode will be generated when  $R=-1$  in presence of a weld penetration rate less than 50%. And with the weld penetration rate increasing, the toe-rib failure mode will be generated instead of the root-weld failure mode.

### 5 Analysis of the Fatigue Testing Program for Objective Failure Mode

On the basis of the results of parametric analyses, fatigue testing program could be determined for generating objective fatigue failure modes, especially for the root-weld and toe-rib failure modes.

The root-deck failure mode could be generated by applying the bending load to the rib-deck welded specimen with an open rib, as shown in Fig. 4. In terms of the specimen with a closed U-rib, it can be concluded from Figs. 11, 12 that the loading mode V combined with the boundary condition A or C should be adopted. However, the toe-deck failure mode might be obtained instead of the root-deck failure since the value of  $\lambda$  thereat is close to the one at the weld root in presence of lower weld penetration rates. Therefore, larger weld penetration rates (*e.g.*, 80% or 100%) should be employed to generate the root-deck failure mode.

The toe-deck failure mode could be obtained by applying the loading mode I (see Fig. 11a) in presence of a weld penetration rate larger than 60%. Non-penetrated rib-deck welded specimen is not recommended even though the toe-deck failure could also be generated, as such penetration rate is rarely applied in practical engineering. Cao et al. (2019) conducted the fatigue test of rib-deck welded specimens with three closed U-ribs, and toe-deck failure mode was

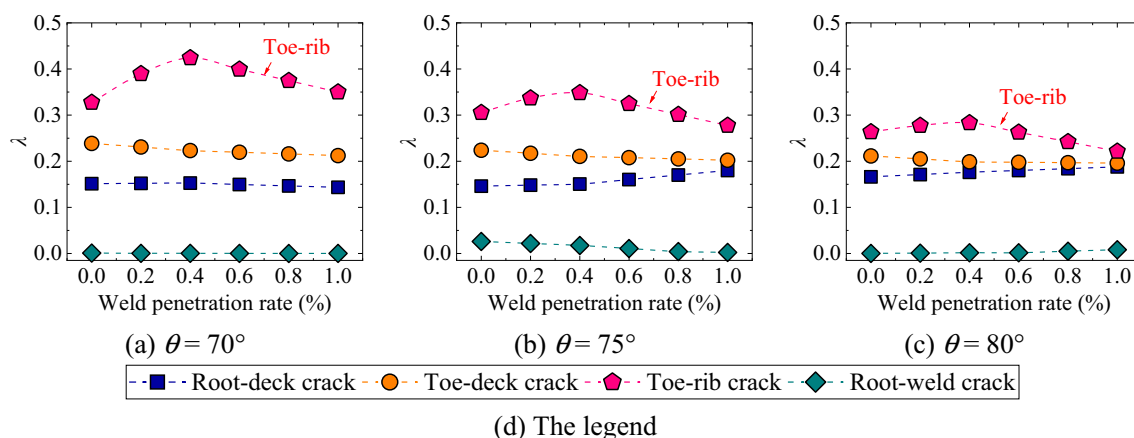
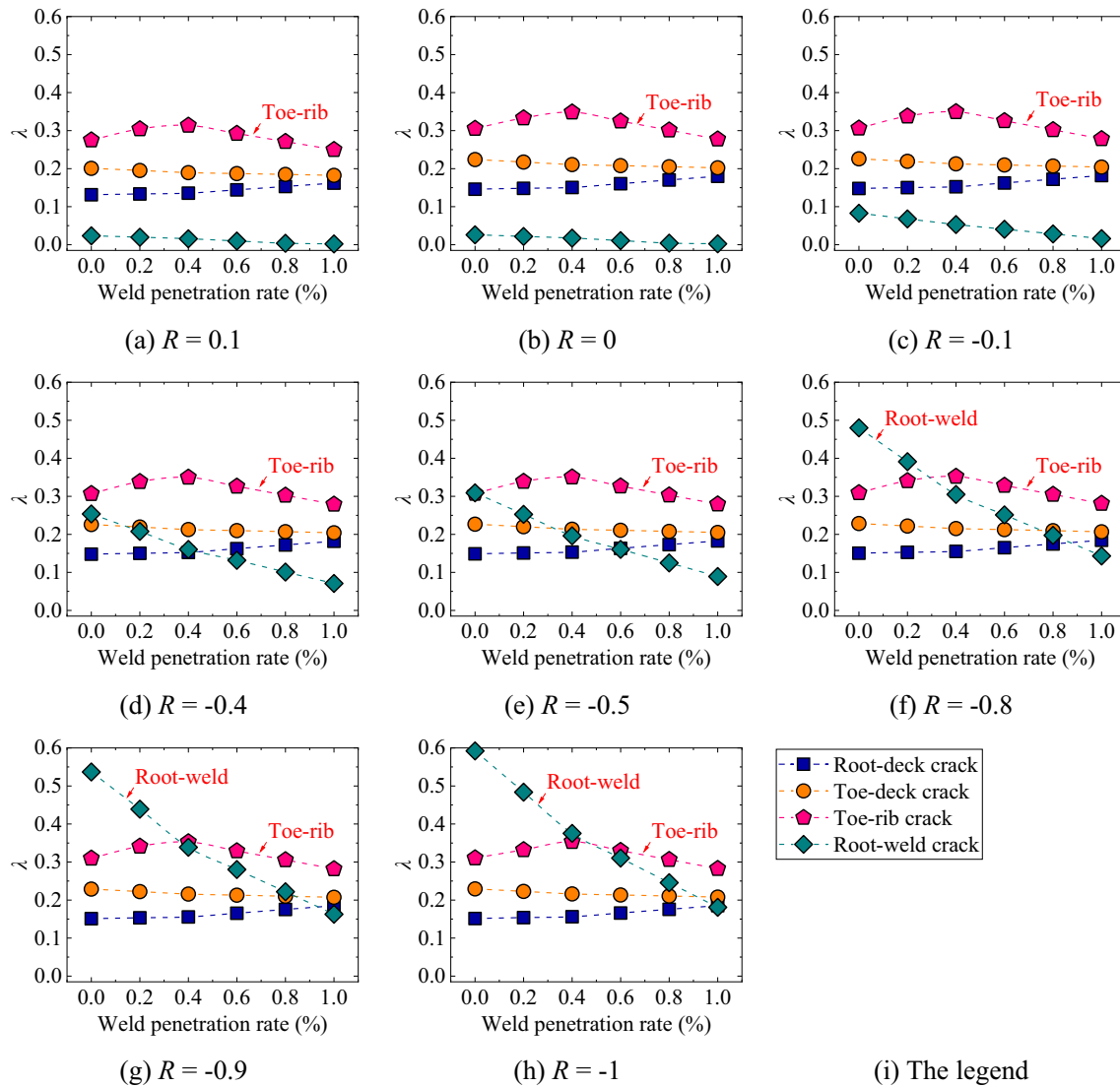


Fig. 15 Effect of  $\theta$  on the value of  $\lambda$  in presence of different weld penetration rates, where  $t_r=6$  mm,  $t_d/t_r=2.0$ ,  $l_{w,d}/t_r=l_{w,r}/t_r=1.0$



**Fig. 16** Effect of stress ratio ( $R$ ) on the value of  $\lambda$  in presence of different weld penetration rates, where  $t_r=6$  mm,  $t_d/t_r=2.0$ ,  $l_{w,d}/t_r=l_{w,r}/t_r=1.0$  and  $\theta=75^\circ$

obtained. In this fatigue test, load transmission beam was employed to apply out-of-plane bending load, which was similar to the loading mode I. Meanwhile, employing the boundary condition B combined with the loading mode II or V is also feasible to generate the toe-deck failure mode. Relative fatigue tests were conducted by Cheng et al. (2017).

For generating the root-weld failure mode, a negative stress ratio smaller than  $-0.5$  combined with a lower weld penetration rate should be adopted (see Fig. 16). It is recommended that the rib-deck welded specimen with a weld penetration rate smaller than 40% should be tested under  $R = -1$ .

The toe-rib failure mode could be obtained by employing the loading mode II, III or IV combined with the boundary condition A or C (see Figs. 11, 12). In this case, a stress

ratio greater than  $-0.5$  should be considered. In view of the feasibility of applying the fatigue load by fatigue testing machine,  $R \geq 0$  is recommended.

## 6 Conclusions

In this study, a simple method for predicting the fatigue failure mode of the rib-deck weld was proposed and validated. Subsequently, parametric analyses were performed to investigate the effects of the loading mode, boundary condition, weld geometry and stress ratio on potential failure mode. On this basis, specific fatigue loading programs for obtaining objective fatigue failure modes were discussed and suggested. The following conclusions can be drawn.

- (1) The parameter  $\lambda$  defined by the ratio of the effective notch stress range ( $\Delta\sigma_0$ ) to the corresponding fatigue strength ( $\Delta\sigma_R$ ) is proposed to predict the fatigue failure mode of the rib-deck weld. Predicting results are in accordance with the three reviewed fatigue tests, indicating well feasibility and reliability of the proposed method.
- (2) The fatigue failure mode of the rib-deck weld is considerably affected by the loading mode, boundary condition and stress ratio induced by external loading. The value of  $l_{w,d}$  affects the failure mode in presence of small weld penetration rates, so is the value of  $t_d$  in presence of full penetration rates. However, the failure mode is independent on the value of  $t_r$ ,  $l_{w,r}$  and  $\theta$ .
- (3) Fatigue testing programs for generating the root-deck, toe-deck, root-weld and toe-rib failure modes of the rib-deck weld are recommended. Suggestions could provide valuable guidance for conducting further fatigue tests to propose the fatigue strength corresponding to the root-weld and toe-rib failure.

**Acknowledgements** This work is sponsored by the Natural Science Foundation of Jiangsu Province (Grant No. BK20220422) and the High-level Scientific Research Foundation for the introduction of talent of Nanjing Forestry University (Grant No. 163050165). The assistance is gratefully acknowledged.

## Declarations

**Conflict of interest** On behalf of all authors, the corresponding author states that there is no conflict of interest.

## References

- AASHTO LRFD (2004) Bridge design specifications, 3rd edn. American Association of State Highway and Transportation Officials, Washington, DC
- Bignonnet A, Jacob B, Caracilli J, LaFrance M (1990) Fatigue resistance of orthotropic steel decks. In: Proceedings IABSE workshop remaining fatigue life of steel structures, Lausanne, Switzerland
- Bruls A (1990) Assessment of fatigue life of orthotropic steel decks. In: Proceedings IABSE workshop remaining fatigue life of steel structures, Lausanne, Switzerland
- Cao BY, Ding YL, Song YS, Zhong W (2019) Fatigue life evaluation for deck-rib welding details of orthotropic steel deck integrating mean stress effects. *J Bridge Eng* 24(2):04018114
- Chen YX, Lv PM, Guo CJ, Li DT, Wang BH (2014) Study on fatigue performance of orthotropic steel bridge deck U-rib and cover weld structure. *J Chang'an Univ (nat Sci Ed)* 34(1):49–55 (in Chinese)
- Cheng B, Ye XH, Cao XE, Mbako D, Cao YS (2017) Experimental study on fatigue failure of rib-to-deck welded connections in orthotropic steel bridge decks. *Int J Fatigue* 103:157–167
- De Freitas S, Kolstein H, Bijlaard F (2017) Fatigue assessment of full-scale retrofitted orthotropic bridge decks. *J Bridge Eng* 22(11):04017092
- Dowling P, Bjorhovde R, Hard J (1992) Constructional steel design-An international guide. CRC Press, London
- Eurocode 3 (2005) Design of steel structures (Part 1–9). European Committee for Standardization, Brussels
- Fisher J, Barsom J (2015) Evaluation of cracking in the rib-to-deck welds of the Bronx-Whitestone bridge. *J Bridge Eng* 21(3):04015065
- Fu ZQ, Ji BH, Zhang CY, Wang QD (2017) Fatigue performance of roof and U-rib weld of orthotropic steel bridge deck with different penetration rates. *J Bridge Eng* 22(6):04017016
- Fu ZQ, Ji BH, Zhang CY, Li D (2018) Experimental study on the fatigue performance of roof and u-rib welds of orthotropic steel bridge decks. *KSCE J Civ Eng* 22(1):270–278
- Heng JL, Zheng KF, Gou C, Zhang Y (2017) Fatigue performance of rib-to-deck joints in orthotropic steel decks with thickened edge U-ribs. *J Bridge Eng* 22(9):04017059
- Hobbacher A (2016) Recommendations for fatigue design of welded joints and components. Springer, Berlin
- Ji BH, Liu R, Chen C, Maeno H, Chen XF (2013) Evaluation on root-deck fatigue of orthotropic steel bridge deck. *J Constr Steel Res* 90(5):174–183
- Kainuma S, Yang MY, Jeong Y (2017) Experimental investigation for structural parameter effects on fatigue behavior of rib-to-deck welded joints in orthotropic steel decks. *Eng Fail Anal* 79:520–537
- Kolstein M (2007) Fatigue classification of welded joints in orthotropic steel bridge decks. PhD thesis, TU Delft
- Li M, Suzuki Y, Hashimoto K, Sugiura K (2018) Experimental study on fatigue resistance of rib-to-deck joint in orthotropic steel bridge deck. *J Bridge Eng* 23(2):04017128
- Maddox S (1974) Fatigue of welded joints loaded in bending. Supplementary Report 84UC, Transport and Road Research Laboratory, Structures Department, Bridges Division, Crowthorne, Berkshire, United Kingdom
- Radaj D (1996) Review of fatigue strength assessment of nonwelded and welded structures based on local parameters. *Int J Fatigue* 18(3):153–170
- Radaj D, Lazzarin P, Berto F (2013) Generalised Neuber concept of fictitious notch rounding. *Int J Fatigue* 51:105–1156
- Rao JH, Ji L, Ji BH (2019) Report on maintenance and operation of Jiangyin Yangtze River Bridge (1999–2019). China Communications Press, Beijing
- Schijve J (2009) Fatigue of structures and materials-Second Edition. Springer, Dordrecht
- Sim H, Uang C, Ya S (2012) Stress analyses and parametric study on full-scale fatigue tests of rib-to-deck welded joints in steel orthotropic decks. *J Bridge Eng* 17:765–773
- Sonsino CM, Fricke W, De Bruyne F, Hoppe A, Ahmadi A, Zhang G (2012) Notch stress concepts for the fatigue assessment of welded joints-background and applications. *Int J Fatigue* 34(1):2–16
- Tian Y, Li YS, Zhang DY, Dai YL (2011) Static and fatigue test research on welded rib-to-deck connections in steel orthotropic bridge deck. *J Railw Sci Eng* 8(2):34–39 (in Chinese)
- Wang QD, Ji BH, Chen X, Ye Z (2019a) Dynamic response analysis-based fatigue evaluation of rib-to-deck welds considering welding residual stress. *Int J Fatigue* 129:105249
- Wang QD, Ji BH, Fu ZQ, Ye Z (2019b) Evaluation of crack propagation and fatigue strength of rib-to-deck welds based on effective notch stress method. *Constr Build Mater* 201:51–61
- Wang DL, Xiang C, Ma YF, Chen AR, Wang BJ (2021a) Experimental study on the root-deck fatigue crack on orthotropic steel decks. *Mat Des* 203:1–15
- Wang QD, Ji BH, Gao T, Fu ZQ (2021b) Effective-notch-stress-based fatigue evaluation of rib-deck welds integrating the full-range S-N curve concept. *J Constr Steel Res* 179:106541
- Wang QD, Wang LB, Ji BH, Fu ZQ (2022) Modified effective notch stress method for fatigue evaluation of rib-deck welds integrating the critical distance approach. *J Constr Steel Res* 196:107373

- Xiao ZG, Yamada K, Ya S, Zhao XL (2008) Stress analyses and fatigue evaluation of rib-to-deck joints in steel orthotropic decks. *Int J Fatigue* 30(8):1387–1397
- Ya S, Yamada K, Ishikawa T (2011) Fatigue evaluation of rib-to-deck welded joints of orthotropic steel bridge deck. *J Bridge Eng* 16(4):492–499
- Yamada K, Ya S (2008) Plate bending fatigue tests for root crack of trough rib of orthotropic steel deck. *JSCE J Struct Eng* 54:675–684 (in Japanese)
- Zhao XX (2010) Research on fatigue design parameter and structural details for orthotropic deck. China Academy of Railway Sciences, Beijing (in Chinese)

Springer Nature or its licensor (e.g. a society or other partner) holds exclusive rights to this article under a publishing agreement with the author(s) or other rightsholder(s); author self-archiving of the accepted manuscript version of this article is solely governed by the terms of such publishing agreement and applicable law.